Modeling and Rheology of HTPB Based Composite Solid Propellants

CEVAT ERİŞKEN,[a] AHMET GÖÇMEZ,[a] ÜLKÜ YILMAZER,[b]
FIKRET PEKEL,[a] and SAIM ÖZKAR*[c]

[a]Defense Industries Research and Development Institute
Tübitak, P.K. 16 Mamak, 06261 Ankara, Turkey

[b]Department of Chemical Engineering
Middle East Technical University
06531 Ankara, Turkey

[c]Department of Chemistry
Middle East Technical University
06531 Ankara, Turkey

The propellant with the minimum viscosity required for a defect-free casting can be obtained by proper selection of the size and fractions of solid components leading to maximum packing density. Furnas' model was used to predict the particulate composition for the maximum packing density. Components with certain size dispersions were combined to yield a size distribution that is closest to the optimum one given by Furnas for maximum packing. The closeness of the calculated size distribution to the optimum one was tested by using the least square technique. The results obtained were experimentally confirmed by viscosity measurement of uncured propellants having HTPB binder and trimodal solid part accordingly prepared by using aluminum (volumetric mean particle diameter of 10.4 μm) and ammonium perchlorate with four different sizes (volumetric mean particle diameters: 9.22, 31.4, 171, and 323 μm). The experimental measurements showed that the compositions for the minimum viscosity are in good agreement with those predicted by using the model for maximum packing. The propellant consisting of particles with mean diameters of 10.4, 31.4, and 323 μm was found to yield the minimum viscosity. This minimum viscosity was observed when the fraction of the sizes with respect to total solids was 0.141, 0.300, and 0.559, respectively.

INTRODUCTION

Composite solid rocket propellant is a heterogeneous mixture of three major ingredients—a polymeric binder, a solid oxidizer, and a metallic fuel. In manufacturing solid propellants, generally, hydroxyl terminated polybutadiene (HTPB), ammonium perchlorate (AP), and aluminum powder (Al) are used as binder, oxidizer, and metallic fuel, respectively. Obtaining high levels of specific impulse and density has been the ultimate goal of propellant development, because these are the major factors affecting the performance of the rocket. As the solid content of the propellant is increased, its density and specific impulse (I_{sp}) increase (1). The increase in the solid content causes first the specific impulse to increase reaching a maximum value at a particular level of loading. Beyond this particular value, it shows a decreasing trend. However, increasing the solid content causes variations in the rheological and mechanical properties of the propellant, too. It is well known that an increase in the solid content results in an increase in the viscosity of the uncured propellant and a decrease in the percent elongation at break of the cured propellant, hence causing difficulties in the processing and failure in the absorption of the stresses in the rocket motor, respectively (2). Thus the solid loading should be increased to such a level that the propellant remains processable while the other properties are still satisfactory.

One way to increase the solid content with a minimal change in the rheological and mechanical properties is to use the concept of packing density, the fraction of voids in a bed that is occupied by solid particles (3). Theory of particle packing is based on the selec-

tion of proper sizes and proportions of particulate material, so that the large voids are filled with particles of matching size, and the new small voids created are in turn filled with smaller particles, and so on. Packing density is influenced by various parameters; the size of particles, the size distribution, shape and surface characteristics of particles, number of component sizes (modality), proportions of components in the mixture, mean diameter ratio of components, interactions between particles, and interactions between particles and suspending fluid (4). There exist theoretical and experimental works in the literature on the packing fraction and general particle dispersion characteristics for arbitrary random packs of spherical particles in suspensions (5-7). In studies on bimodal concentrated suspensions, for example, the fluidity has been found to decrease with the increasing solid content, but to increase with an increase in the packing density at a specified solid content (7). Although the particle size and fraction have been found to affect, and used to control, the burning characteristics of the propellant (8) as well as the packing density, the challenge in this field is to pack as much ammonium perchlorate and aluminum particles as possible within a unit volume of propellant.

Here we report on development of a model that gives the composition of particulates leading to maximum packing density in obtaining a propellant with minimum viscosity at a certain level of solid loading. Based on the assumption that Furnas' theory (9) is applicable for aluminum and ammonium perchlorate particles, the fraction of each solid component that yields a size distribution closest to the optimum one was determined. The deviation between the optimum size distribution and the size distribution obtained by the model was minimized. The developed model was tested by rheological characterization of the uncured propellants with the predetermined fractions of components. Using the sizes available, trimodal propellant blends were prepared according to results of the model and tested together with the other compositions around the model predictions to observe the effect of size fraction of particles in each size on propellant rheology. Based on the results obtained in this work, we also studied the mechanical and burning rate properties of propellants with various sizes, fine-coarse ratio, and solid loading (10).

Model for Obtaining the Fractions of Solids for Maximum Packing

The first theoretical approach for the prediction of optimum size distribution was proposed for mixtures with continuous size distribution by Furnas (9) who derived relations between the specific volume (defined as the inverse of apparent density) and composition of ideal binary mixtures. He used the partial specific volume of the coarse and fine components to elucidate the concepts and to show a simple graphic procedure for representing the relation. This graphic procedure

has been improved and extended to the study of idealized packing of spheres of different sizes (11, 12). Although Furnas' theory was shown to have some discrepancies when compared with experimental results of dry mixtures (13), it can yield feasible results when applied to a solid mixture wetted with a polymer matrix. The following expression is given by Furnas for the calculation of the ratio, r, (large to small) of the amount of materials on two consecutive screens.

$$r^{\frac{m-1}{n-1}} = \frac{1}{V} \quad or \quad r = \frac{1}{V^{\frac{n-1}{m-1}}} \tag{1}$$

where n is the number of component sizes, m is the number of screens with a successive size ratio of 1.21, and V is the compositional average of the void fractions of component sizes. The void fraction of each component size must be known or experimentally determined to predict the optimum size distribution for maximum packing density by using the following procedure:

1. Select the size range to be used and obtain the screen sizes differing by a ratio of 1.21
2. Decide on the number of component sizes, n, to be used
3. Find the ratio of weight or volume in a continuous series for particles having the same true density by using *Eq 1*.
4. Taking the amount of material for the finest size as 1, determine the amount of succeeding size by multiplying the previous amount by a factor of r. This yields the optimum size distribution.

The procedure described is very helpful in determining the optimum distribution of particles for maximum packing and yields a cumulative distribution of particle sizes.

Determination of Fractional Volumes of Components With Different Sizes

Furnas' method is a common way of approaching the maximum packing value and optimum size distribution, yet it does not explain how to prepare a mixture that will yield maximum packing. It is all right if one is planning to use m number of fractions and all the fractions consist of monodispersed particles that are uniform in size. If this were the case, one would take the amounts of fractions determined by the ratio r and mix them for a sufficient period of time to get the maximum attainable packing. However, when the number of component sizes is not equal to m, and they are distributed over a range, preparation of a mixture becomes somehow difficult. Furnas actually gives a plot of the number of the fractions versus the ratio of the diameter of the smallest particle to the diameter of the largest particle. Using this plot, he determines the number of component sizes to be combined. However, one may desire to use as many fractions as possible or the ratio of diameters may not fall

in a reasonable range. For a trimodal mixture ($n = 3$) used in this study, there is a corresponding cumulative percent distribution, $F(D)$, which can be obtained from the cumulative size distribution of the component n under particle size D, $F_n(D)$, and the fraction of components, x_n ($n = 1, 2, 3$), by using Eq 2.

$$F(D) = \sum_{n=1}^{3} x_n F_n(D) \qquad (2)$$

Table 1 summarizes such a cumulative distribution in a general system of n components. $O(D)$ is the optimum cumulative distribution under the particle size D. Equation 2 gives the model cumulative percentage of the particles under size D, corresponding to the same screen number in the optimum case. For attaining the maximum packing density, the model and optimum particle size distribution, $F(D)$, and $O(D)$, respectively, should be as close as possible to each other. This can be tested by applying the common least square method. The sum of the squares of the differences between the optimum and the model cumulative size distributions in each screen size m is set to be minimum.

$$S = \sum_{1}^{m} [F(D_m) - O(D_m)]^2 \qquad (3)$$

For the particular case of three components with the fractional volumes x_1, x_2, and x_3, this requires

$$\frac{\partial S}{\partial x_1} = 0, \ \frac{\partial S}{\partial x_2} = 0, \ \frac{\partial S}{\partial x_3} = 0 \qquad (4)$$

Fractional volumes of the components that will give the maximum packing density can be obtained from the simultaneous solution of these differential equations by using simple mathematical tools.

EXPERIMENTAL

Materials: HTPB (R-45M, number average molecular weight of 2700 g/mol, functionality of 1.93, Arco Chemical Company, Philadelphia); Isophoron diisocyanate, IPDI, (Fluka AG, Leverkusen, Germany); crystalline ammonium perchlorate (AP, average particle sizes of 31.4 µm, 171 µm, and 323 µm SNPE, France), aluminum powder (average particle size of 10.4 µm Alcan Toyo) were used as purchased. Sizes of solid particles were measured by using a Malvern Mastersizer Model MSX. Packing the particles as dense as

possible is achieved by using a Heinz Janetzki K.-G. T-5 Centrifuge having four cylindrical sample units. The tubes are of 23 mm in inner diameter and 90 mm in height. Ammonium perchlorate with the average particle size of 9.22 µm was produced by grinding the coarse ammonium perchlorate of 171 µm size in a laboratory mill (Alpine, Type 160 Z).

Void Fraction Determination: The void fractions of samples were determined by compressing the particles in the centrifuge. Solid particles to be analyzed were first dried in the oven at 110°C before measurements were taken. Eighty grams of dried sample from one selected size was transferred into four tubes in equal amounts, and the top surfaces of the samples were smoothed for ease of leveling. The tubes were then inserted into the cells of the centrifuge and rotated at a speed of 5500 rpm for 15 minutes. After this period of time, the tubes were taken out and the level of the sample was marked. The apparent volume of particles was then determined by filling the empty tubes with distilled water, with the aid of a burette, up to the marked level of particles.

Combinations of the Solid Component Sizes: Six different sets were selected to obtain the size distribution closest to the optimum distribution of the model. These sets are trimodal combinations containing aluminum and two of four ammonium perchlorates available in different sizes as given below:

Set 1: Al (10.4 µm), Fine AP (9.22 µm), Coarse AP (31.4 µm)

Set 2: Al (10.4 µm), Fine AP (9.22 µm), Coarse AP (171 µm)

Set 3: Al (10.4 µm), Fine AP (9.22 µm), Coarse AP (323 µm)

Set 4: Al (10.4 µm), Fine AP (31.4 µm), Coarse AP (171 µm)

Set 5: Al (10.4 µm), Fine AP (31.4 µm), Coarse AP (323 µm)

Set 6: Al (10.4 µm), Fine AP (171 µm), Coarse AP (323 µm)

Propellant Mixing Equipment and Procedure: Propellant mixing was carried out in a 1 gallon Baker Perkins vertical mixer. Control of temperature is critical during the process because reactions are taking

Table 1. Cumulative Distribution in a General System of n Components.

Particle Diameter	Size Distribution of Components (Cumulative Percent Undersize)					Optimum Size Distribution	Model Size Distribution
(D)	$F_1(D)$	$F_2(D)$	$F_3(D)$	...	$F_n(D)$	O(D)	F(D)
D_1	$F_1(D_1)$	$F_2(D_1)$	$F_3(D_1)$	...	$F_n(D_1)$	$O(D_1)$	$F(D_1)$
D_2	$F_1(D_2)$	$F_2(D_2)$	$F_3(D_2)$	...	$F_n(D_2)$	$O(D_2)$	$F(D_2)$
.	.	.	.	.	.	.	.
.	.	.	.	.	.	.	.
.	.	.	.	.	.	.	.
D_m	$F_1(D_m)$	$F_2(D_m)$	$F_3(D_m)$	$F_4(D_m)$	$F_n(D_m)$	$O(D_m)$	$F(D_m)$

place. Hot water was circulated through the jacket of the mixer so that the suspension was kept at a temperature of 65 ± 1°C. All the liquid ingredients except the curing agent were premixed thoroughly for about 10 min at 65°C. The mixing was then continued under vacuum for about 3 hours upon addition of solid components. Finally, the curing agent IPDI was added to the slurry, the mixture was blended for another 15 min at 65°C.

Viscosity Measurements: The instrument used in viscosity measurements was a rotational type digital Brookfield Viscometer Model HBTDV-II. Viscosity measurements were carried out according to ASTM Standard D 2196-81. For measuring the viscosity, a 500 ml sample of uncured propellant slurry at 65°C was transferred into a beaker and put in the water bath, which was at 65°C. The spindle, which was previously conditioned at 65°C, was attached to the lower shaft of the viscometer while it was in the propellant slurry. The spindle was centered in the test fluid and immersed to a marked level of the T-spindle. The rotational speed was adjusted to the slowest value of 0.5 rpm. Viscosity first increased up to a maximum value and then decreased. When the highest value appeared, the timer was started and readings were recorded every 10 seconds up to the end of four revolutions. This time is 480 seconds for 0.5 rpm. The same procedure was repeated for 1, 2.5, 5, 10, 20, and 100 rpm, and the viscosity was recorded.

RESULTS AND DISCUSSIONS

Calculation of Void Fractions

Determination of the void fractions of each component is very critical, because the optimum size distribution is highly affected by the average void fractions

of component sizes (*Eq 1*). The void fractions of the components were calculated from the apparent volumes of the component sizes measured by applying centrifugation which provides ease of use and high repeatability of the results. To test the repeatability of the method, four measurements were performed for each component size of 20 g sample. Once apparent volume is measured, the apparent density can be calculated by dividing the mass of the sample by its apparent volume. Void fraction can then be determined by using *Eq 5*.

$$Void\ fraction = 1 - \frac{\rho_{app}}{\rho_p} \tag{5}$$

where ρ_{app} and ρ_p are apparent and particle densities, respectively. The void fractions for all component sizes are given in *Table 2* together with the standard deviations which are not remarkable. Inspection of the results shows that the average void fraction decreases with increasing average particle diameter. The increase in void fraction with decreasing particle diameter may be attributed to the changes in particulate interactions with size (14). Static electrical forces, friction, adhesion, and other surface forces become increasingly important as particle size decreases, and the surface area to volume ratio is markedly increased. However, it is hard to find a relationship between the mean particle diameter and the void fraction because the particles are polydispersed in size and shape, different from the monodispersed glass beads that were used for the model studies (14).

Calculation of the Fractions of the Solid Component Sizes

The size distribution closest to the optimum distribution can be obtained if the appropriate fractions of

Table 2. Void Fractions of Components Measured on 20 g Samples After Applying Centrifugation.

Average Diameter (μm)	Vol. (cm³)	Apparent Density (g/cm³)	Particle Density (g/cm³)	Void Fraction	Average Void Fraction	Standard Deviation of Void Fractions
323 (AP)	15.8	1.266	1.95	0.3509	0.374	0.019
	16.5	1.212	1.95	0.3784		
	16.3	1.227	1.95	0.3708		
	17.0	1.176	1.95	0.3967		
171 (AP)	17.3	1.156	1.95	0.4071	0.409	0.004
	17.5	1.143	1.95	0.4139		
	17.4	1.149	1.95	0.4106		
	17.2	1.163	1.95	0.4037		
31.4 (AP)	17.8	1.124	1.95	0.4238	0.417	0.005
	17.5	1.143	1.95	0.4139		
	17.5	1.143	1.95	0.4139		
	17.6	1.136	1.95	0.4172		
9.22 (AP)	24.4	0.820	1.95	0.5797	0.587	0.007
	25.0	0.800	1.95	0.5897		
	24.6	0.813	1.95	0.5831		
	25.3	0.791	1.95	0.5946		
10.4 (Al)	13.9	1.439	2.7	0.4671	0.438	0.021
	13.2	1.515	2.7	0.4388		
	12.7	1.575	2.7	0.4167		
	13.0	1.538	2.7	0.4302		

Fig. 1. Particle size distribution in a trimodal mixture: Calculated by using Eq 2 and experimentally measured.
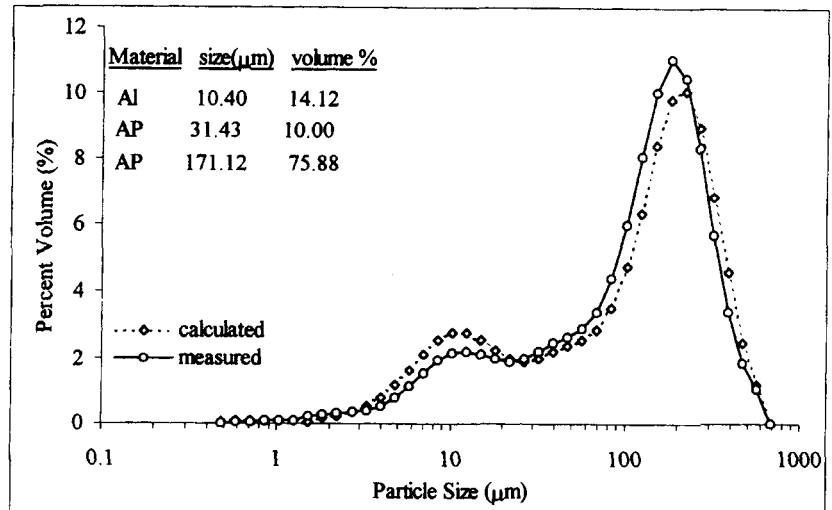
the solid components are determined by some means. In practice, this idea is applicable by means of Eq 2. To check the validity of Eq 2, arbitrary values of x_n were selected and the distribution of the mixture was determined for each screen size by using Eq 2. Then, a mixture was prepared with the selected proportions of solid components and its particle size distribution was measured. As an example, a trimodal mixture of ammonium perchlorate (10.00% of 31.4 µm, 75.88% of 171 µm) and aluminum particles (14.12%) was prepared and the size distribution of the mixture was measured and calculated by using Eq 2. Both the measured and calculated distributions are depicted in Fig. 1. The closeness of these two distributions clearly indicates that Eq 2 can be used to determine the size distribution of a multimodal mixture if the size distribution of its components are known.

Using the void fractions of solid components given in Table 2, the optimum size distributions were obtained by using the aforementioned procedure. The smallest screen size is 0.48 µm and the succeeding screens have sizes 1.21 times that of the preceding screen size. The largest screen size is 683 µ, and the total number of screens is 39. All the mixtures prepared are trimodal, having one aluminum and two different ammonium perchlorate solid component sizes. Table 3 illustrates an example of the calculation of optimum size distribution in a trimodal mixture containing one aluminum and two ammonium perchlorate solid components (9.22 µm and 171 µm) by following the procedure given before. The calculated optimum cumulative percent undersize distributions are given in Table 4 for all the trimodal mixtures containing one aluminum and two ammonium perchlorate solid components. Please recall that the optimum distributions in Table 4 provide the maximum packing densities of the mixtures.

The size distribution obtained by using the model should be closest to the optimum size distribution. In

Table 3. Calculation of Optimum Cumulative Size Distribution in a Trimodal Mixture Containing One Aluminum and Two Ammonium Perchlorate Components (9.22 µm and 171 µm) by Following the Procedure.

Diameter (µm)	Amount (volumetric)	Volume %	Cumulative Distribution (%)
0.48	1.00	1.04	1.04
0.59	1.04	1.08	2.12
0.71	1.09	1.13	3.24
0.86	1.13	1.17	4.42
1.04	1.18	1.22	5.64
1.26	1.23	1.28	6.92
1.52	1.29	1.33	8.25
1.84	1.34	1.39	9.64
2.23	1.34	1.45	11.1
2.7	1.46	1.51	12.6
3.27	1.52	1.58	14.2
3.95	1.59	1.64	15.8
4.79	1.66	1.71	17.5
5.79	1.73	1.79	19.3
7.01	1.80	1.86	21.2
8.48	1.88	1.94	23.1
10.3	1.96	2.03	25.2
12.4	2.04	2.11	27.3
15.1	2.13	2.20	29.5
18.2	2.22	2.30	31.7
22.0	2.32	2.40	34.2
26.7	2.42	2.50	36.7
32.3	2.52	2.61	39.3
39.1	2.62	2.72	42.0
47.3	2.74	2.84	44.8
57.3	2.86	2.30	47.8
69.3	2.98	3.08	50.9
83.9	3.11	3.22	54.1
101	3.24	3.35	57.4
122	3.38	3.50	60.9
148	3.52	3.65	64.6
180	3.68	3.81	68.4
218	3.83	3.97	72.4
264	4.00	4.14	76.5
319	4.17	4.32	80.8
386	4.35	4.50	85.3
467	4.53	4.69	90.0
565	4.73	4.89	94.9
683	4.93	5.10	100.0

Table 4. Optimum Cumulative Size Distribution in a Trimodal Mixture Containing One Aluminum and Two Ammonium Perchlorate Components Calculated by Following the Procedure.

Diameter (μm)	Al 10.4 μm AP 9.22 μm AP 31.4 μm	Al 10.4 μm AP 9.22 μm AP 323 μm	Al 10.4 μm AP 9.22 μm AP 171 μm	Al 10.4 μm AP 31.4 μm AP 171 μm	Al 10.4 μm AP 31.4 μm AP 323 μm	Al 10.4 μm AP 171 μm AP 323 μm
	Cumulative Percent Undersize Distribution					
0.48	1.15	1.04	1.04	0.93	0.89	0.93
0.59	2.37	2.13	2.12	1.91	1.82	1.90
0.71	3.66	3.26	3.24	2.93	2.80	2.91
0.86	5.02	4.44	4.42	4.00	3.82	3.98
1.04	6.46	5.68	5.64	5.12	4.90	5.10
1.26	7.99	6.96	6.92	6.29	6.03	6.26
1.52	9.60	8.28	8.25	7.52	7.21	7.49
1.84	11.3	9.69	9.64	8.81	8.45	8.77
2.23	13.1	11.2	11.1	10.1	9.76	10.1
2.7	15.0	12.7	12.6	11.6	11.1	11.5
3.27	17.0	14.3	14.2	13.1	12.6	13.0
3.95	19.2	15.9	15.8	14.6	14.1	14.5
4.79	21.4	17.6	17.5	16.2	15.7	16.2
5.79	23.8	19.4	19.3	17.9	17.3	17.9
7.01	26.3	21.3	21.2	19.7	19.1	19.6
8.48	29.0	23.3	23.1	21.6	20.9	21.5
10.3	31.8	25.3	25.2	23.5	22.8	23.4
12.4	34.8	27.4	27.3	25.6	24.8	25.5
15.1	37.9	29.6	29.5	27.7	27.0	27.6
18.2	41.3	31.9	31.7	30.0	29.2	29.9
22.0	44.8	34.3	34.2	32.3	31.5	32.2
26.7	48.6	36.8	36.7	34.8	34.0	34.7
32.3	52.5	39.4	39.3	37.4	36.5	37.3
39.1	56.7	42.1	42.0	40.1	39.2	40.0
47.3	61.1	44.9	44.8	42.9	42.0	42.8
57.3	65.8	47.9	47.8	45.9	45.0	45.8
69.3	70.7	51.0	50.9	49.0	48.1	48.9
83.9	75.9	54.2	54.1	52.2	51.4	52.1
101	81.4	57.6	57.4	55.6	54.8	55.6
122	87.3	61.1	60.9	59.2	58.4	59.1
148	93.5	64.7	64.6	62.9	62.2	62.9
180	100	68.5	68.4	66.9	66.2	66.8
218	100	72.5	72.4	71.0	70.3	70.9
264	100	76.6	76.5	75.3	74.7	75.2
319	100	80.9	80.8	79.8	79.3	79.7
386	100	85.4	85.3	84.5	84.1	84.4
467	100	90.0	90.0	89.4	89.1	89.4
565	100	94.9	94.9	94.4	94.4	94.6
683	100	100	100	100	100	100

other words, the deviation between the two distributions should be minimum (*Eq 3*). When the differentiations of the sum S with respect to x_n are set to be equal to zero for the minimum value of S (*Eq 4*), the fractions of the solid component sizes can be determined. *Equation 3* is composed of 39 terms, each containing a second order polynomial. This equation was differentiated and solved by using the Mathcad Package. The fractions of the solid components calculated for the maximum packing of six different trimodal mixtures by integration of *Eq 4* are given in *Table 5*. The volume fractions of the solid components calculated for maximum packing density in this way were used in *Eq 2* to obtain the model size distribution for

Table 5. The Fractions of the Solid Components Calculated for the Maximum Packing of Trimodal Mixtures by Integration of Eq 4.

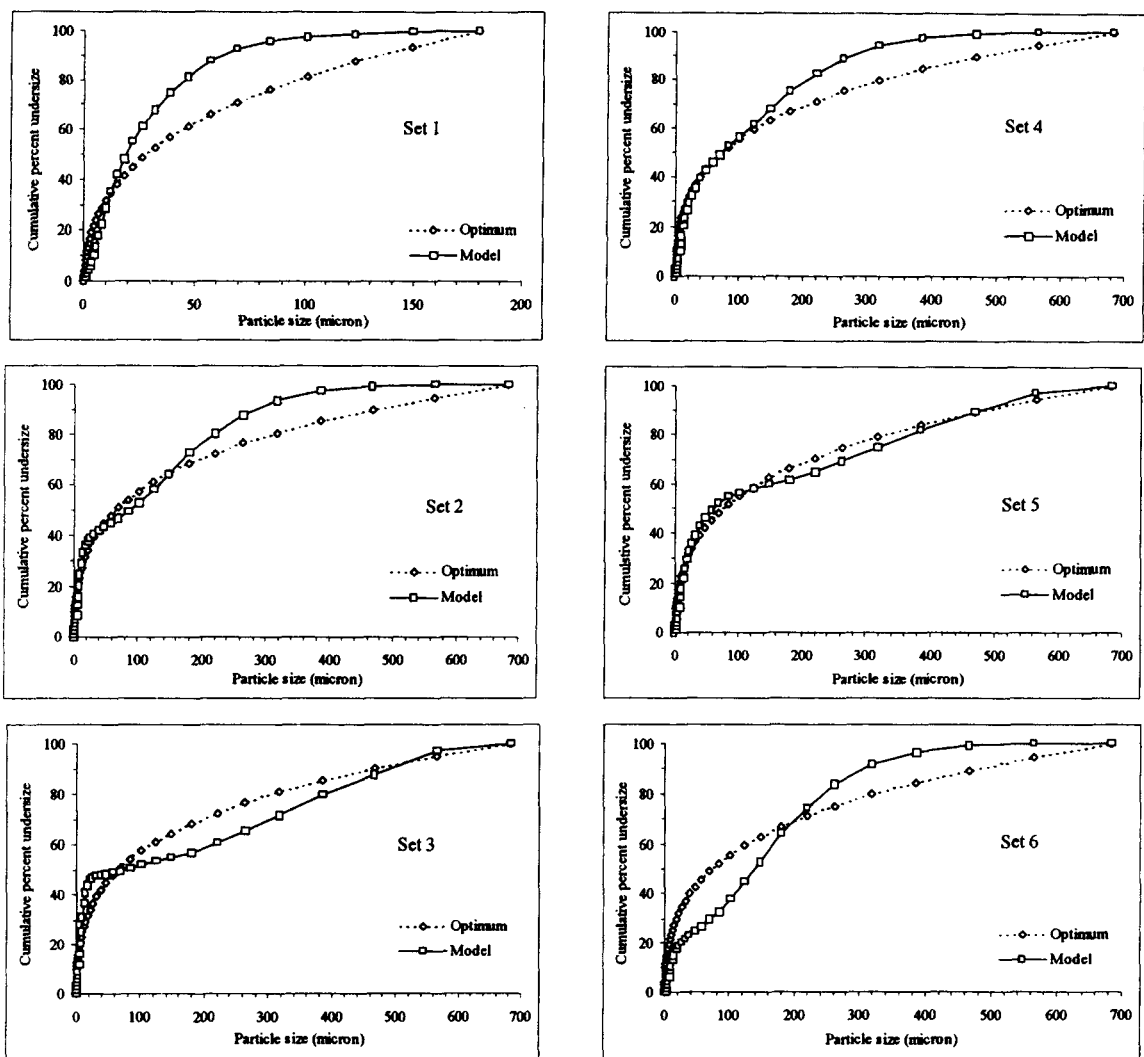| Set No.	Volume Fractions of Component Sizes				
	Al, 10.4 μm	AP, 9.22 μm	AP, 31.4 μm	AP, 171 μm	AP, 323 μm
1	0.14	0.01	0.85	—	—
2	0.14	0.22	—	0.64	—
3	0.14	0.32	—	—	0.54
4	0.14	—	0.27	0.59	—
5	0.14	—	0.38	—	0.48
6	0.14	—	—	0.86	0.00

Fig. 2. Comparison of the optimum size distributions with those predicted by modeling for trimodal mixtures of sets 1–6.

each set. The deviation of the model size distribution from the optimum size distribution can be easily visualized from the graphs obtained (*Fig. 2*). For set 1, there exists a gap for the particle diameters between 25 μm and 150 μm, indicating that some particles of sizes in this range should be removed to increase the packing density of the mixture. Similar gaps also exist in the other sets. For sets 2 and 4, some of the particles having sizes between 200 μm and 550 μm should be taken out of the mixture, while sets 3 and 6 require the addition of particles in certain range for maximum packing. The least deviation from the optimum size distribution is observed for set 5. From the inspection of the plots of the size distributions for all the trimodal mixtures, set 5 is found to have the most suitable size distribution for the maximum packing density. The packing densities for the remaining sets can be ranked in the decreasing order 3 > 2 > 4 > 1 > 6. The largest deviation is observed for sets 1 and 6. For this reason, these combinations were not prepared for

rheological characterization, since they would exhibit high viscosity.

Results of Rheological Measurements

The propellant slurries containing 75% (87% by weight) one of the sets 2, 3, 4, and 5 as solid loading were prepared and characterized rheologically. The viscosity of the propellant slurry shows variations with time. To illustrate the thixotropic behavior of the propellant slurries, the time-dependent viscosity at 0.5 rpm for the slurry containing 75% (by volume) the trimodal mixture of the set 2 is depicted in *Fig. 3*. Muthiah *et al.* (15) observed a similar oscillatory behavior for the viscosity of the hydroxyl terminated polybutadiene propellant slurry in the time range between 160 and 200 min. However, the overall effect was an increase in viscosity of the propellant slurry with time, owing to the curing reaction. The oscillatory behavior of the slurry viscosity in *Fig. 3* is not attributed to the build-up of the network by curing since the duration
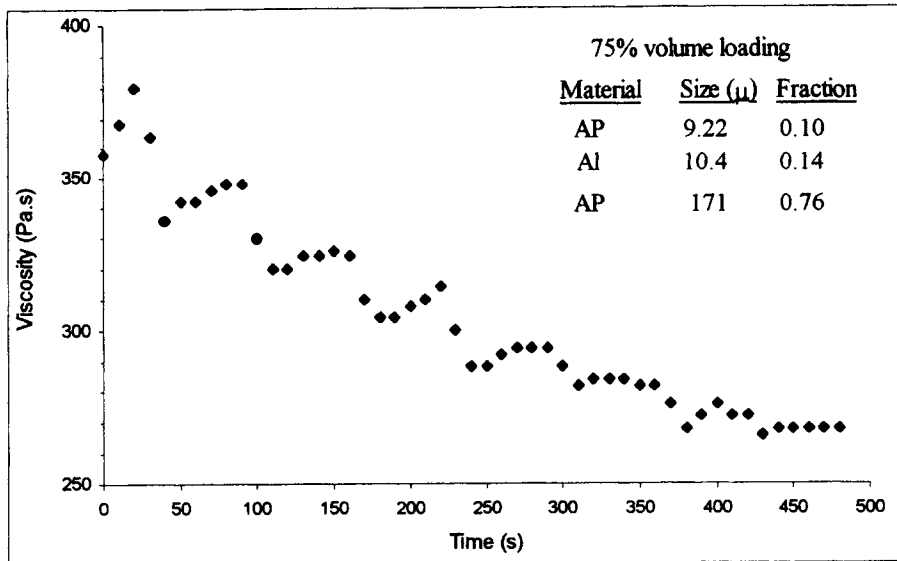
Fig. 3. Time-dependent viscosity at 0.5 rpm for the slurry containing 75% (by volume) a trimodal mixture of set 2.

of our experiments (less than 8 min) is much smaller than that reported by Muthiah et al. (15). Instead, the oscillatory nature of the slurry viscosity is due to the formation of the agglomerates, followed by breakdown, which is caused by the effect of shear. An overall shear thinning effect was dominant in the time range in which the measurements were taken. The period of the oscillations also increases with the time. In the experiments, recording of data was ceased after four revolutions of the spindle. The number of revolutions was kept constant at all spindle speeds to avoid the incorporation of any additional experimental parameter. Although the use of Brookfield viscometer is not the best technique to measure the viscosity of the propellant slurries, the data collected could be used to compare the viscosity of uncured propellants with vari-

ous compositions, not to determine their rheological characteristics.

Table 6 gives the slurry viscosity of the propellants containing the trimodal solid mixtures of sets 2–5 depending on the volume fraction of fine AP in the solid loading and on the shear rate. The viscosity values in Table 6 represent the last reading at each rpm value, i.e., reading taken after four revolutions of the spindle. Figure 4 shows the variation in the slurry viscosity of the propellant with the shear rate. The results given in Fig. 4 are in agreement with the results reported by Osgood (16), who observed a pseudoplastic flow behavior of the propellant. Because of the complexity of the flow behavior of the uncured propellants, it is very difficult to make a comparison between the results of different propellants. The flow behavior is

Table 6. The Slurry Viscosities of the Propellants Containing the Trimodal Solid Mixtures of Sets 2–5 Depending on the Volume Fraction of Fine AP in the Solid Loading and on the Shear Rate.

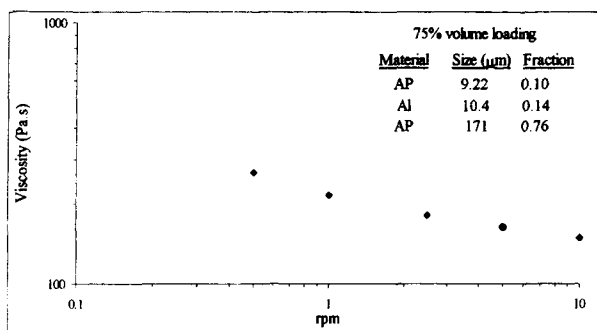| Set No.	Volume Fraction of Fine AP	Viscosity (Pa·s)				
		0.5 rpm	1 rpm	2.5 rpm	5 rpm	10 rpm
2	0.10	268	216	181	166	159
	0.24	86	80	78	77	78
	0.40	138	126	123	129	141
3	0.04	125	101	82	72	69
	0.15	70	64	56	54	52
	0.33	70	66	65	67	69
	0.50	147	138	135	143	154
4	0.10	352	259	176	126	83
	0.27	118	109	100	97	93
	0.40	106	99	96	95	94
	0.52	122	117	115	116	117
5	0.15	61	51	47	45	43
	0.30	54	48	45	44	44
	0.40	54	53	50	51	51
	0.55	83	82	82	83	85

Fig. 4. Variation in the slurry viscosity of the propellant with the shear rate.

usually characterized by using the viscosity values measured at low shear rates. Among the results given in *Table 6*, the viscosity values recorded at a shear rate of 2.5 rpm were selected for comparison. Another reason for this selection is the requirement of the applied percent torque that is proportional to the applied shear stress, which is around 10% of the maximum range for the Brookfield Viscometer to be used efficiently. This requirement could be fulfilled by viscosity measurements at 2.5 rpm for all the propellants.

The concept of packing fraction can be used to understand the changes in the slurry viscosity of propellants with the fractions of the components in the solid part. For this purpose, the following relation between the viscosity and packing fraction has been proposed by Maron and Pierce (17).

$$\eta_r = \left(1 - \frac{\varphi}{\varphi_p}\right)^{-2} \tag{6}$$

where η_r is the relative viscosity defined as the ratio of the suspension viscosity to the suspending medium viscosity, φ is the total volume fraction of solids in the slurry, and φ_p is the maximum packing fraction of the system at a specified total solid content. *Equation 6* shows that viscosity is a function of the total volume fraction of the solids and the maximum packing fraction at this loading level. The relative viscosity is expected to decrease with the increasing maximum packing fraction of the system at constant loading (18).

Figure 5 shows the effect of compositional variation on the relative viscosity of the propellant slurry. The relative viscosities in *Fig. 5* were determined by dividing the viscosity of the slurry by the viscosity of the unfilled polymer matrix (6.4 Pa·s at 2.5 rpm). It is seen that the relative viscosity of propellant slurries first decreases with the increasing volume fraction of fine AP and then increases after passing through a minimum. A second order polynomial trend line was fitted to the experimental data points for an accurate determination of the fraction giving this minimum viscosity. For set 2, for instance, the volume fraction of fine AP giving minimum viscosity is 0.28. The packing fraction (φ_p) of the solids mixture increases until the volume fraction of the fine AP (9.22 μm) reaches the value of 0.28. The viscosity of the slurry containing these particles decreases because (φ/φ_p) decreases (*Eq 6*). At the point where the fraction of the fines is 0.28, the packing fraction of the system reaches its maximum attainable value and (φ/φ_p) becomes minimum. At this point, φ_p is equal to φ_{max}. After this point, φ_p begins to decrease with further increase in the fraction of fines. The relative viscosity at maximum packing condition is equal to 12 for the propellant slurry containing the trimodal solid mixture of set 2. In this
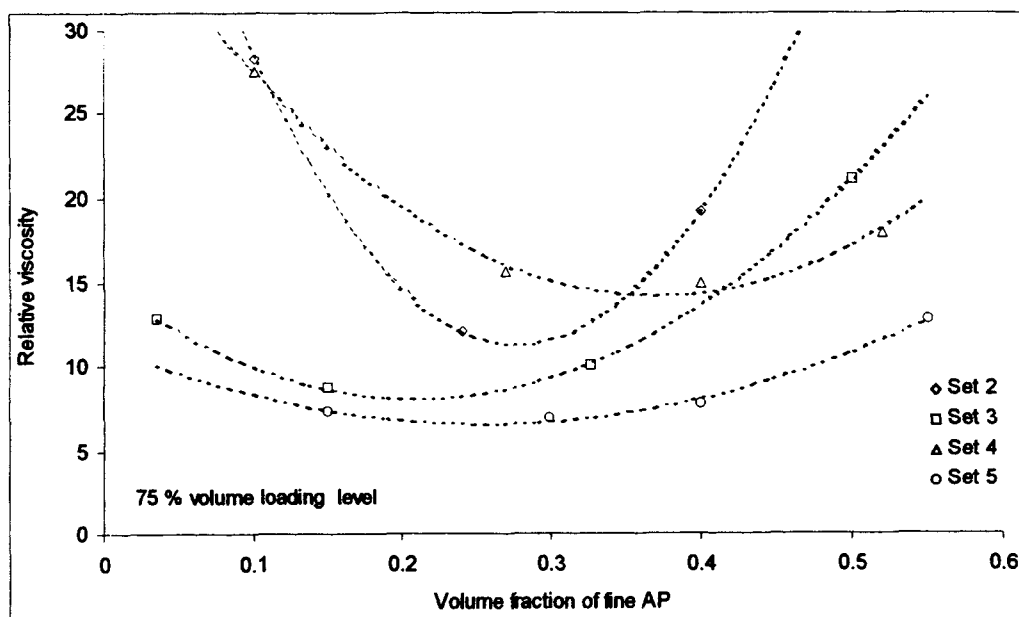

Fig. 5. Effect of fraction of the fine AP in the total solids on the relative viscosity of the propellant slurry measured at 2.5 rpm.

Cevat Erişken, Ahmet Göçmez, Ülkü Yılmazer, Fikret Pekel, and Saim Özkar

Table 7. Volume Fractions of Component Sizes of a Trimodal Solid Mixture Containing One Aluminum and Two Ammonium Perchlorate Components, Calculated by Modeling for Maximum Packing Density and Determined by Rheological Measurements for Minimum Viscosity.

| Set No. | Volume Fractions of Component Sizes | | | | | | | | | | Percent Deviation |
| | 9.22 μm | | 10.4 μm | | 31.4 μm | | 171 μm | | 323 μm | | |
	Model	Exp	Model	Exp	Model	Exp	Model	Exp	Model	Exp	
2	0.22	0.28	0.14	0.14			0.64	0.58			10
3	0.32	0.20	0.14	0.14					0.54	0.66	18
4			0.14	0.14	0.27	0.36	0.59	0.50			18
5			0.14	0.14	0.38	0.30			0.48	0.56	14

way, the volume fractions of the solid components giving the minimum viscosity and the corresponding minimum viscosity can be determined for all the propellant slurries containing trimodal solid mixtures of sets 2–5 at maximum packing conditions.

CONCLUSION

The volume fractions of the solid components experimentally determined by viscosity measurements are given in *Table 7* together with the values estimated by modeling for maximum packing density. The results resemble the prediction of the Farris method for the fine:medium:coarse ratio of ~20:30:50 in highly concentrated suspensions (6) if one remembers that in most of our blends the medium and fine particles (aluminum and fine ammonium perchlorate) are not very different in size, but in the origin. Indeed, the minimum viscosity was yielded by the propellant consisting of particles with mean diameters of 10.4 μm, 31.4 μm, and 323 μm, whereby the particle sizes are the mostly separated ones among the used materials. This minimum viscosity was observed when the fraction of the sizes with respect to total solids was 0.141, 0.300, and 0.559, respectively.

The last column in *Table 7* shows the deviation of the model from the experimental values. The deviation was calculated with respect to the fractions of the coarse AP particles of the minimum viscosity propellant. A maximum of 18% deviation from the experimental results was observed. Although this is acceptable for engineering applications, the reasons causing the deviation are to be explained from a scientific point of view. The latter requires further investigation in more detail. However, some error sources can be mentioned here.

The main reason for the deviation may be the shapes of the particles. The solid particles used in propellant manufacturing have irregular shapes except for the aluminum powder, while the Furnas' method that gives the optimum particle size distribution was developed for spherical particles. The void fractions used as inputs for the optimum size distribution were determined by dry mixing of the particulates, which may yield inaccuracy in the measurements, for the solid particles cannot be perfectly mixed in dry conditions.

Similar studies for maximum packing have been performed using particles with very large diameters compared with the particles used in this study. Furnas' method has been tested only for particles with large diameters (in the order of millimeters), such as sand, aggregates, etc. On the other hand, the maximum particle diameter in this study is less than 600 μm. Although no restriction was given by Furnas in terms of particle diameter, the deviation of the model may also be due to the small particle sizes.

REFERENCES

1. N. Kubota, "Survey of Rocket Propellants and Their Combustion Characteristics," in K. K. Kuo and M. Summerfield, eds, *Fundamentals of Solid-Propellant Combustion*, pp. 1–52, American Institute of Aeronautics and Astronautics Inc., New York (1984).
2. J. S. Chong, E. B. Christiansen, and A. D. Baer, *J. Appl. Polym. Sci.*, **15**, 2007 (1971).
3. D. P. Haughey and G. S. G. Beveridge, *Canadian J. Chem. Eng.*, **47**, 130 (1969).
4. A. B. Yu and N. Standish, *Powder Technol.*, **76**, 113 (1993).
5. I. L. Davis and R. G. Carter, *J. Appl. Phys.*, **67**, 1022 (1990).
6. R. J. Farris, *Trans. Soc. Rheology*, **12**, 281 (1968).
7. A. P. Shapiro and R. F. Probstein, *Phys. Rev. Lett.*, **68**, 1422 (1992); R. F. Probstein, M. Z. Sengun, and T. C. Tseng, *J. Rheol.*, **38**, 811 (1994); M. Z. Sengun and R. F. Probstein, *J. Rheol.*, **41**, 811 (1997).
8. L. Zivorad, *J. Propulsion*, **6**, 515 (1990).
9. C. C. Furnas, *Ind. Eng. Chem.*, **23**, 1052 (1931).
10. A. Göçmez, C. Erişken, Ü. Yılmazer, F. Pekel, and S. Özkar, "Mechanical and Burning Properties of Highly Loaded Composite Propellants," *J. Appl. Polym. Sci.*, **67**, 1457 (1998).
11. R. K. McGeary, *J. Am. Ceramic Soc.*, **44**, 513 (1961).
12. G. L. Messing and G. Y. JR. Onada, *J. Am. Ceramic Soc.*, **61**, 363 (1978).
13. H. Y. Sohn and C. Moreland, *Canadian J. Chem. Eng.*, **46**, 162 (1968).
14. R. J. Wakeman, *Powder Technol.*, **11**, 297 (1975).
15. R. M. Muthiah, R. Manjari, V. N. Krishnamurty, and B. R. Gupta, *Polym. Eng. Sci.*, **31**, 61 (1991).
16. A. A. Osgood, "Rheological Characterization of Non-newtonian Propellants for Casting Optimization," *AIAA paper no* **69-518**, 1–5 (1969).
17. S. H. Maron and P. E. Pierce, *J. Colloid Sci.*, **11**, 80 (1956).
18. R. K. Gupta and S. G. Seshadri, *J. Rheol.*, **30**, 503 (1986).